Induced Seismicity in pressurised single fractures: a numerical approach

Sismicidad inducida en fracturas presurizadas: una aproximación numérica

Guillem Piris[1], Albert Griera[2], Enrique Gomez-Rivas[3], Ignasi Herms[1] and Xavier Goula[1]

[1] Institut Cartogràfic i Geològic de Catalunya (ICGC), Parc de Montjuic, s/n, 08038 Barcelona, Spain. piris_de_casau@hotmail.com; ignasi.herms@icgc.cat; xavier.Goula@icgc.cat

[2] Departament de Geologia, Universitat Autònoma de Barcelona, E-08193 Bellaterra (Cerdanyola del Vallès), Spain. albert.griera@uab.cat

[3] School of Geosciencies, King's College, University of Aberdeen, AB24 3UE Aberdeen, United Kingdom. e.gomez-rivas@abdn.ac.uk

ABSTRACT

The exploration and exploitation of deep geothermal reservoirs has significantly increased during the last years. These reservoirs use heat exchange to produce heat or electricity. The so-called Enhanced Geothermal Systems (EGS) are characterized by a stimulation phase that aims to increase fluid flow and heat transfer between wells by increasing the permeability and transitivity of the reservoir. This is achieved by injecting high-pressure fluids (normally water) in order to increase the apertures of existing fractures, enhancing their sliding and/or generating new ones. However, this technique induces low-magnitude seismicity that occasionally results in damage at the Earth's surface. Numerical simulations able to reproduce the hydro-thermo-mechanical behaviour of geological reservoirs are an essential tool for the evaluation and forecasting of induced seismicity in such systems. In this study, the numerical code CFRAC is used to systematically evaluate how the orientation of faults with respect to the stress field influences seismicity, the injection rate and the fracture sliding behaviour.

Key-words: *Geothermal reservoir, induced seismicity, modelling, fracture orientation, slip regime.*

RESUMEN

La exploración y explotación de reservorios geotérmicos profundos se ha incrementado significativamente durante los últimos años. Los Sistemas Geotérmicos Estimulados (EGS) requieren de una fase de estimulación para incrementar el flujo de fluidos y la transferencia de calor entre pozos mediante el incremento de la permeabilidad y la transmisividad en el reservorio. Esto se consigue inyectando fluidos a alta presión para aumentar la apertura de las fracturas preexistentes, facilitar su deslizamiento y/o crear nuevas fracturas. Esta técnica presenta la desventaja de que puede producir sismicidad inducida de baja magnitud que, en ocasiones, puede producir daños en superficie. Las simulaciones numéricas del comportamiento termo-hidro-mecánico de reservorios geológicos durante la fase de inyección de fluidos pueden ayudar a la evaluación y predicción de la sismicidad inducida en estos casos. En este trabajo, se usa el código numérico CFRAC para evaluar de forma sistemática la influencia que la orientación de las fracturas con respecto el campo de esfuerzos tiene en la sismicidad, el caudal de inyección y el comportamiento de deslizamiento.

Palabras clave: *Reservorio geotérmico, sismicidad inducida, modelización, orientación de las fracturas, régimen de deslizamiento.*

Geogaceta, 61 (2017), 95-98
ISSN (versión impresa): 0213-683X
ISSN (Internet): 2173-6545

Recepción: 15 de julio de 2016
Revisión: 3 de noviembre de 2016
Aceptación: 25 de noviembre 2016

Introduction

The exploration and exploitation of deep geothermal reservoirs has significantly increased in recent years worldwide. These reservoirs are generally located in crystalline basement rocks that present high geothermal gradients and a low-permeability typically controlled by natural fracture networks. Heat and/or electricity can be produced from these reservoirs by exchanging heat between fluids and host rocks. Two types of deep geothermal resources can be distinguished: (i) hydrothermal, which use a pre-existing hot water aquifer and (ii) petrothermal, or Enhanced Geothermal Systems (EGS), which are characterized by low-permeability, dry crystalline rocks that require a phase of hydraulic stimulation (Gnatus *et al.,* 2010).

The hydraulic stimulation phase in EGS improves the permeability of the reservoir by reworking the pre-existent fracture network or by generating new fractures. The stimulation process can raise reservoir permeability by an order of magnitude or more (Gnatus *et al.,* 2010). A serious issue related to hydraulic stimulation is that it can result in induced seismicity (Majer *et al.,* 2007). This type of seismicity is called micro seismicity due to the low resulting magnitude. The monitoring and control of this induced seismicity is a key challenge for the public acceptance and viability of EGS projects. There have been several cases of moderate magnitude seismicity associated with initial stages of stimulation projects during the last years (e.g. see summary in Dempsey and Suckale, 2015).

An accurate prediction of the induced seismicity phenomena associated with hydraulic stimulation and the development of strategies for risk governance are essential for the viability of EGSs. This requires the development of tools capable of simulating

the thermo-hydro-mechanical response of fractured geological reservoirs during fluid injection.

In this study, we explore this issue by means of a series of numerical simulations focussed on the evolution of single fracture systems. The dependence of fracture orientation with respect to the stress field orientation is systematically evaluated in terms of event production, injection rates, sliding behaviour and fluid pressure evolution.

Methods

The numerical models were carried out with the discontinuous element code CFRAC (Complex ReseArch Code v 1.3; McClure, 2012). The code is specifically designed to address problems related to fluid injection into a fractured rock medium and the associated induced seismicity. The fully coupled thermo-hydro-mechanical problem is solved for fractures, which can either open or slide. The main equations for solving the mass balance, fluid flow or for solving the fracture aperture and sliding are described in McClure (2012).

The friction coefficient is evaluated using the rate and state friction law (Scholz, 2002), and it is defined as a function of two variables: the sliding velocity (v) and the past sliding history of the fracture or state (θ_{RS}),

$$\mu_f(v,\theta) = f_o + a\cdot \ln\left(\frac{v}{v_o}\right) + b\cdot \ln\left(\frac{\theta_{RS}\, v_o}{d_c}\right) \quad (1)$$

where, f_0 is the friction coefficient for a reference sliding velocity v_0, d_c is the critical distance that has relation with the fracture rugosity, a and b are fracture material parameters and finally, θ_{RS} is the state variable.

The code also integrates a process that allows simulating the production of seismic events. A microseismic event is considered to begin when the sliding velocity along a fracture exceeds a reference velocity of 5 mm/s. A slip event is considered finished when the highest velocity in the fracture drops below 2.5mm/s (McClure, 2012). The hypocenters of these microevents are located in the element where the reference sliding velocity is exceeded first. The seismic moment magnitude and the seismic moment are defined according to the size of the event. The seismic moment (M_0) is defined as a function of the fracture area and its displacement. The seismic moment magnitude (M_w) is estimated following the empirical law by Hanks and Kanamori (1979).

Geometry and Models

The boundary conditions for all models were selected to be similar to those produced during the crisis of the Basel EGS reservoir (Gischig, 2015). The geothermal reservoir was assumed to be at a depth of 4,500 m with a hydrostatic fluid pressure gradient. The principal stresses σ_1 and σ_3 were horizontal, while σ_2 was vertical (strike-slip regime).

The initial fracture properties and the *rate-and-state* frictional model were set with similar values than those by Gischig (2015) in his mechanical analysis of the Basel reservoir (Table I). The model contained a 600 m long single isolated fracture embedded in a 2D space. The fluid was injected at the centre of the fracture, with a constant pressure in the head well of 75 MPa. The investigated parameter was the influence of the fracture orientation (θ, defined as the angle between the principal compressive stress σ_1 and the fault normal) on the induced seismicity, injection rates, sliding behaviour and fluid pressure accommodation. 21 models were run with θ ranging between 15º and 88º.

Results

Figure 1 summarizes the simulation results. The sliding velocity (m/s), fluid pressure (MPa), injection rate (kg/s) and event magnitude evolution along fracture distance and elapsed time (s) are shown for the more representative cases (with θ=88º, 86º, 76º and 60º). The locations of the seismic event hypocentres were superposed to the fluid pressure fields (indicated with white dots in Fig. 1 E, H and K). Most of the seismic events were not located at the highest fluid pressure regions, but at the pressurised fronts where the maximum gradient of fluid pressure was observed.

For the case of a single fracture oriented at a high angle (θ=88º; Fig. 1A-C) a linear and homogenous expansion of the pressurised front from the injection point towards the fracture end points was observed. High-pressure values (p_f=75 MPa) were observed along a large part of the fracture, with a discrete and sharp pressurised front. Sliding velocities were homogenous and ranged approx. from 10^{-7} to 10^{-5} m/s, implying that no seismic events were generated. Deformation or slip along the fracture was aseismically accommodated. Very low injection rates were obtained (<< 5 Kg/s; Fig. 1C).

h	Off-plane dimension	100 m
f_0	Nominal friction coefficient	0.85
d_c	Critical distance	100 µm
a	Velocity effect coefficient	0.01
b	State effect coefficient	0.02
v_0	Reference velocity	10^{-6} m/s
θ_{RS}	State	2.6x10^6s

Table I. Friction parameters and off-plane dimension used in the simulations.

Tabla I. Parámetros de fricción y dimensión fuera de plano utilizados en las simulaciones.

The θ=86º model showed a similar fluid pressure evolution than the previous one, but with higher sliding velocities (up to 10^{-4} - 10^{-3} m/s) and relatively sudden variations of slip velocities (Fig. 1D-F). Seismic events were found at centre and away from the pressurised front. Dynamic ruptures associated with these events never able to overcome the pressurized front. The event magnitudes increased with the elapsed injection time, up to a maximum of Mw~2. In some cases, injection rates attained values of 10 kg/s, although there was a decreasing tendency after the maximum peak was reached (Fig. 1F).

Fluid pressure in the θ=76º model showed a continuous gradient between the injection point and the pressurized front (Fig. 1G-I). The sliding velocities were characterised by abrupt and discrete high velocities (max. 10^{-2} to 10^{-0} m/s), which expanded quickly along the fracture. None of the observed events implied dynamic ruptures along the whole fracture distance. The overall fracture ruptures were normally observed following two consecutive seismic events. Local accelerations of the sliding velocities were observed from the hypocenters to the fracture margins, acting as precursors for instabilities. The events were located at the front of the pressurized zone and dynamic ruptures expanded outside of the pressurised zone. Seismic magnitudes slowly increased together with the expansion of the pressurized zone. Injection rates attained values of 60 kg/s in some cases, followed by a fast decrease to reach a stationary value of about 10 kg/s (Fig. 1I).

The θ=60º model revealed that a small patch of fluid pressure was enough to induce high-sliding velocity events (Fig. 1 J-L). Surface ruptures, or propagation of high sliding velocities, was not restricted by fluid pressure and propagated along all the fracture section. Therefore, a small pressure perturbation was able to critically produce rup-

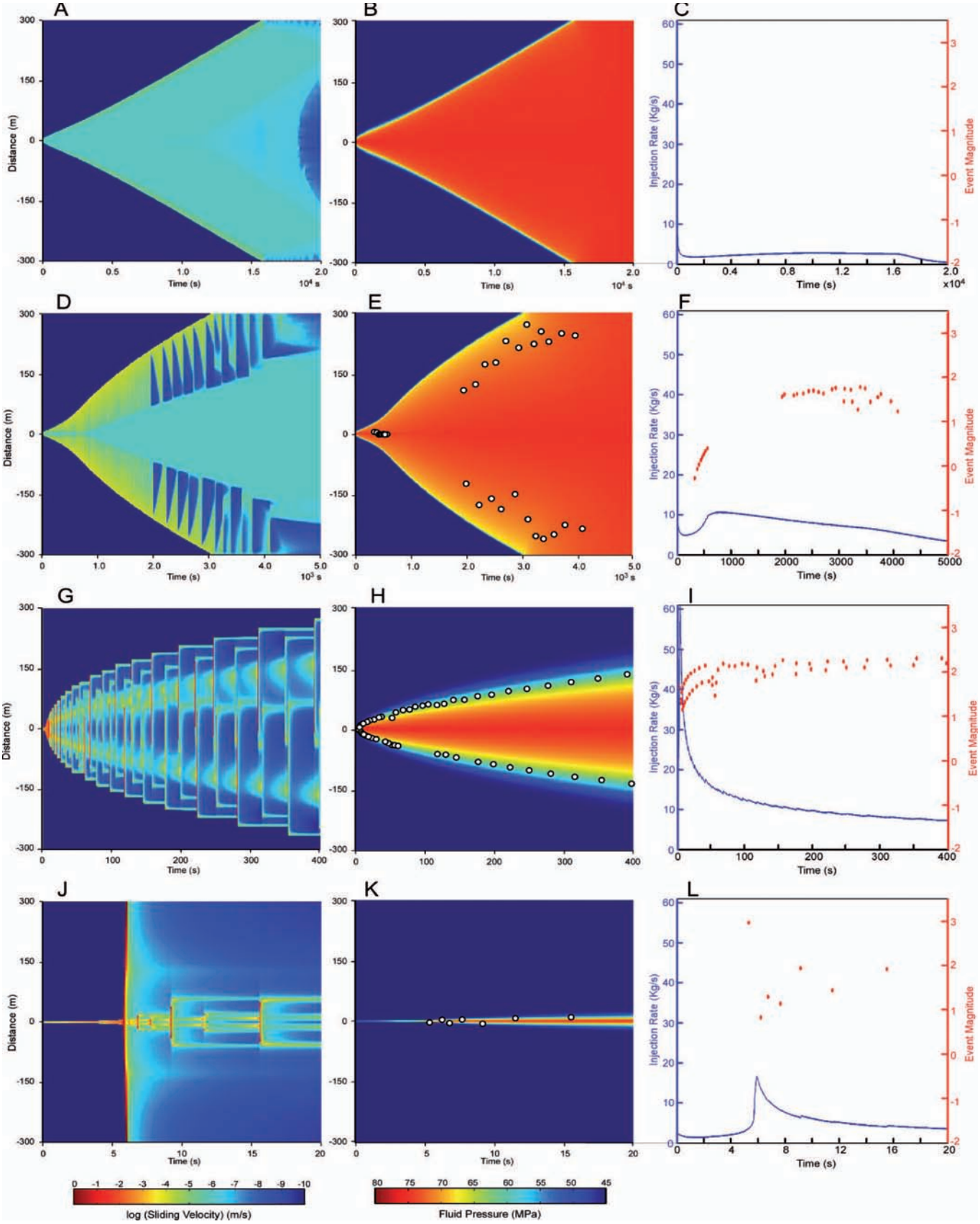

Fig 1. Sliding velocity (m/s), fluid pressure (MPa), injection rate (kg/s) and event magnitude evolution along fracture distance and time elapsed (s) for model θ =88° (A-C), θ =86° (D-F), θ =76° (G-I) and θ =60°(J-L). White points indicate hypocentre of seismic events. See color figure in the web.

Fig 1. Velocidad de deslizamiento (m/s), presión de fluido (MPa), caudal de inyección (kg/s) y la evolución de los seísmos a lo largo de la fractura y el tiempo transcurrido (s) para los modelos θ =88° (A-C), θ =86° (D-F), θ =76° (G-I) and θ =60°(J-L). Los puntos blancos indican la localización hipocentral de los seísmos. Ver figura en color en la web.

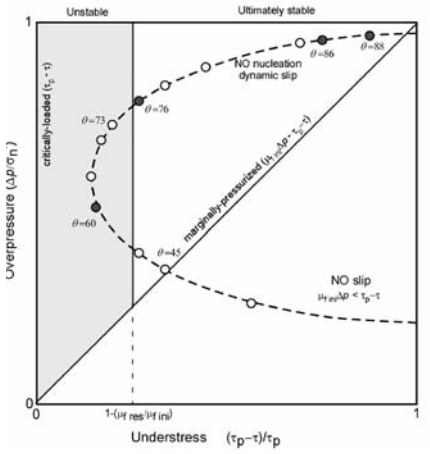

Fig. 2. Slip regimes as a function of the overpressure and understress field. The dark dashed line represents the evolution trajectory as a function of the fracture orientation (from θ=0° to θ=90°). White points indicate models done but do not shown. Grey dark points are simulations shown in Fig. 1. Δp is the fluid pressure increment, σ'_n is the effective normal stress, τ_p is the critical shear stress to slip and τ the shear stress on a plane. Modified from Garagash and Germanovich (2012).

Fig 2. Regímenes de deslizamiento en función de los campos de overpressure y understress. La línea negra discontinua representa la trayectoria de evolución en función de la orientación de la fractura (de θ=0° a θ=90°). Los puntos blancos indican modelos realizados pero no mostrados. Los puntos gris oscuro son las simulaciones mostradas en la Fig.1. Δp es el incremento de presión de fluido, σ'_n es la tensión normal efectiva, τ_p es la tensión tangencial de deslizamiento crítica y τ es la tensión tangencial para un plano dado. Modificada de Garagash y Germanovich (2012).

ture along the entire fracture plane. For this case, the event with the highest magnitude *Mw* ~ 3 was correlated with the maximum injection rate, near a peak value of 20 kg/s that was followed by a progressive decrease until reaching 5 kg/s approx (Fig. 1L).

Discussion

The results show that the seismic behaviour during injection is strongly influenced by the fracture orientation, at least for single-fracture cases. Three main seismic regimes can clearly be distinguished. The first type are events that do not require a large fluid overpressure patch on the fracture before the onset and nucleation of a seismic event. A small perturbation of strength is enough to produce a critical load and fracture reactivation. The size of the rupture surface is larger than the size of the pressurised patch, and therefore, slip along the fracture can expand outside of the pressurised front leading to situations of uncontrolled rupture propagation. The fractures oriented between θ=50º and θ=76º follow this behaviour.

The second type of response is defined by fracture orientations that require longer injection times before the onset of fracture slip. In this case, the onset of dynamic slip requires that a large part of the fracture is first uniformly pressurised. Seismic events in this case are not located near the injection point, but into the pressurised front. They are characterised by high slip velocities and surface run-outs that can expand outside of the pressurised region, but are still able to produce rupture surface along the whole fracture distance. This implies that, although the dynamic slip behaviour is efficient and there is weakening of the friction coefficient, the residual friction must be high enough to arrest and stabilise the perturbation. The fracture orientation ranges between $76º \leq \theta < 85º$ and $45º \leq \theta \leq 50º$.

Finally, a third case with the fracture oriented $\theta \geq 85º$ can be defined. In this case, dynamic slip is not observed and fracture propagation is arrested due to the increase of the dynamic friction coefficient during the raise of the slip velocity (see eq. 1). The accommodation of loading, and therefore the accommodation of a finite displacement along the fracture, takes place by means of slow motion events (i.e. low-magnitude seismicity) or by aseismic flow (i.e. at velocities lower than the predefined by the threshold for seismic events).

These three slip regimes are coherent with the analytical model by Garagash and Germanovich (2012) on the nucleation and arrest of dynamic slip on a pressurised fault and numerical simulations by Gischig (2015). Garagash and Germanovich (2012) proposed a different way for predicting the slip regime behaviour using a diagram defined by the understress versus the overpressure (Fig. 2). For the stress conditions simulated in our models the data show that the condition of no slip corresponds to fractures with an angle of $0º \leq \theta < 45º$, the critically loaded regime takes place for angles $50º < \theta < 76º$, the marginally pressurised scenario corresponds to angles between $45º \leq \theta \leq 50º$ and $76º \leq \theta < 85º$, and, finally, fractures oriented $\theta \geq 85º$ result in aseismic or no dynamic slip (or low seismic magnitude events). The transition between the last two cases is difficult to define because it is a function of the critical distance d_c, related physically with the fracture rugosity.

Conclusions

The orientation of single fractures with respect to the stress field is a key factor controlling induced seismicity. For the conditions simulated in the models, three different slip regimes were observed: (1) critically loaded regime, (2) marginally pressurised regime and (3) no dynamic slip or aseismic. The production of seismic events, sliding regime and fluid pressure distribution vary according to the slip regime or fracture orientation.

Acknowledgments

We would like to thank M.W. McClure for providing the CFRAC code used in this work. The Institut Cartogràfic i Geològic de Catalunya is acknowledged for their support. We thank Sergio Llana-Fúnez and José Luis Simón for comments which improved the manuscript.

References

Dempsey, D. and Suckale, J. (2015). Induced Earthquakes Sequences in Geothermal Settings: Data Trends and Modeling Approaches. PROCEEDINGS, Fortieth Workshop on Geothermal Reservoir Engineering. Stanford University, Stanford, California. SGP-TR-204.

Garagash, P. and Germanovich, L. N. (2012). Nucleation and arrest of dynamic slip on a pressurized fault. *Journal of Geophysical Research*, 117, B10310.

Gischig, V. S. (2015). Rupture propagation behavior and the largest possible earthquake induced by fluid injection into deep reservoirs. *Geophysics Research Letters*, 42, 7420–7428.

Gnatus, N. A., Khutorskoy, M. D. and Khmelevskoi, V. K. (2010). Petrothermal Energy and Geophysics. Moscow University Geology Bulletin, vol. 66, No. 3, pp. 151-157.

Hanks, T. and Kanamori, H. (1979). A moment magnitude scale. *Journal of Geophysical Research*, 84, 2348–2350.

Majer, E., Baria, R., Stark, M., Oates, S., Bommer, J., Smith, B. and Asanuma, H. (2007). Induced seismicity associated with enhanced geothermal systems. *Geothermics*, 36 (3), 185–222.

McClure, M. W. (2012). *Modeling and Characterization of Hydraulic Stimulation and Induced Seismicity in Geothermal and Shale Gas Reservoirs*, PhD dissertation, Stanford University, Stanford, California, 349 p.

Scholz, C. H. (2002). *The Mechanics of Earthquakes and Faulting*, Cambridge University Press, Cambridge, 471p.